

# Systems Medicine 2020 Lecture Notes

Uri Alon

## Lecture 10

### Aging and the saturation of damage removal

We've just seen some basic facts about aging on the population level, such as the Gompertz law. We also discussed how different forms of molecular damage cause aging, in part through the accumulation of senescent cells. In this lecture we connect between the molecular and population levels. To do so, we will build a conceptual framework to understand the stochastic processes of senescent cell accumulation and removal. Our payoff will be a first-principle explanation of the Gompertz law, of increasing variation in aging, and of the dynamics of aging interventions.

#### Senescent cell dynamics show nearly exponential rise with age and lengthening correlation times

We saw that **senescent cells** are an important accumulating factor that is causal for aging: removing senescent cells slows aging whereas adding them increases risk of death. It makes sense, then, to explore how the amount of senescent cells in the body, which we denote by  $X$ , varies with age in different individuals.

For simplicity, we will pretend that senescent cells are a single category, despite the fact that they are likely to be a name for many different cell states and cell types, accumulating in the different organs of the body. For organisms without senescent cells, such as *C. elegans* and fruit flies, we will think of  $X$  as a type of damage, such as protein damage, that is a primary cause for aging.

To get a feeling for the dynamics of senescent cells, let's consider an experiment, by (Burd et al., 2013), who measured senescent cell abundance in 33 mice every 8 weeks for 80 weeks. To measure whole-body senescent cell amounts, Burd et al used genetic engineering to produce mice that made photons in proportion to the number of senescent cells they have (Fig 10.1). In a nutshell, they used a gene from fireflies called **luciferase** that produces photons when it acts on a certain

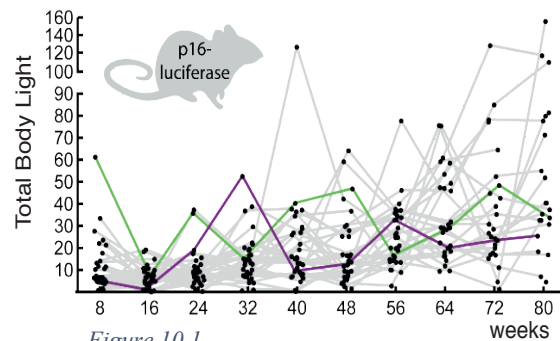


Figure 10.1

substrate. They introduced the luciferase gene into the mouse DNA, and placed it under the control of a DNA element, called the p16 promoter, that is normally activated only in senescent cells. Therefore, only the senescent cells in these mice make the protein luciferase. When the substrate for this protein is injected into the mouse, the mice produce light. Mice normally don't make photons, so that observing the light emitted from their special mice allowed Burd et al to estimate senescent cell abundance,  $X$ . The experiment has several limitations, such as stronger absorption of light from inner regions, some genetic disruption of the natural p16 system which enhanced the chance of cancer after 80 weeks so the experiment could not probe very old ages, and experimental noise. But the experiment serves as a good starting point.

Looking at total light emitted from these mice as a measurement of  $X$ , we see that  $X$  rises and falls across time and generally increases with age (Fig 10.1).

The data suggests two timescales: fast timescale of fluctuations over weeks, and a slow timescale in which  $X$  rises on average over years (Fig 10.2). This fast-slow timescale separation will be useful for building our model.

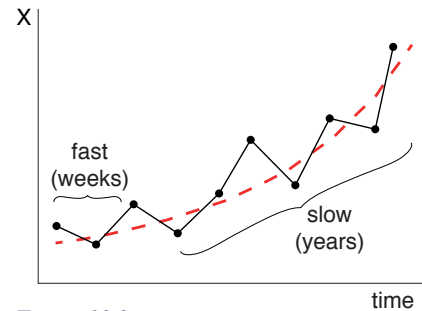


Figure 10.2

Analyzing the data provides four features:

- (i) The *average  $X$  grows at an accelerating rate* nearly-exponentially with age (Fig 10.3). It looks nearly exponential. Such nearly-exponential accumulation with age is also seen in senescent cells in human tissues.
- (ii) The *variation in  $X$  between individuals grows with age* (Fig 10.3). Old mice have a larger range of  $X$  than young mice. Some old mice even have  $X$  levels similar to young mice (Fig 10.1). This variation grows, however, more slowly than the growth of average: the mean  $X$  divided by standard deviation grows roughly linearly with age  $\frac{\langle X \rangle}{std(X)} \sim \tau$  (Fig 10.4 inset).

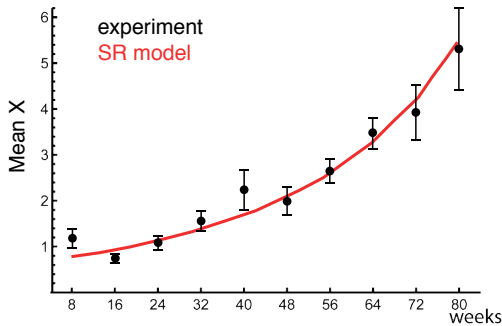


Figure 10.3

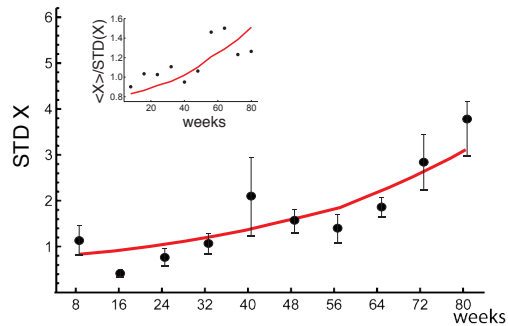


Figure 10.4

(iii) Distributions of  $X$  among individuals at a given age are skewed to the right, so that there are more individuals with higher than average  $X$  than

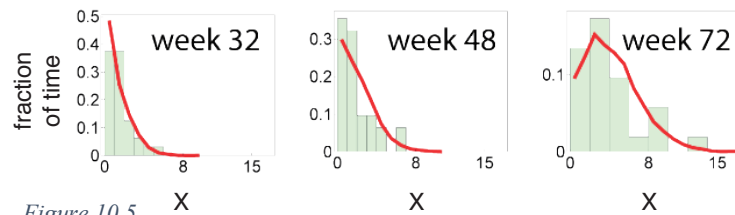


Figure 10.5

individuals with lower than average  $X$  (Fig 10.5). The skewness of these distributions gradually drops with age.

(iv) The correlation time of  $X$  increases with age. This means that a mouse that is higher or lower than average stays so for longer periods of time at old age than at young ages. (Fig 10.6).

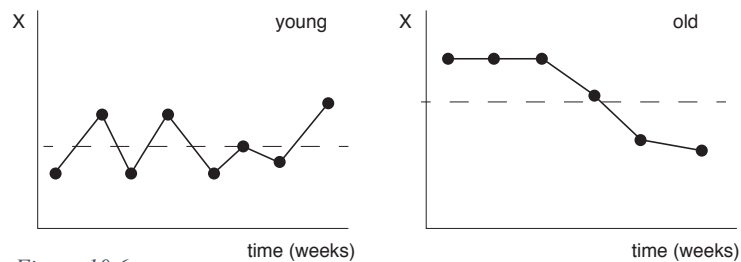


Figure 10.6

Thus, with age, the stochastic variation in  $X$  becomes more persistent.

Interestingly, these features are shared with the human frailty index described in the last lecture, which also rises exponentially with age, shows widening variation (increasing standard deviation) with age that rises more slowly than the mean, and skewed distributions between individuals.

### A model with increasing production and saturating removal can explain senescent-cell dynamics

These dynamical features of senescent cells can be explained by a simple model, called the **saturating removal (SR)** model, as discovered by Omer Karin in his PhD with me. Omer scanned a wide class of models, and found the essential features that a model needs in order to explain the senescent cells dynamics we just discussed.

The first important feature is to have **two timescales**, a fast and a slow timescale:  $X$  is produced and removed on a timescale that is much faster than the lifespan. This separation of timescales allows us to write an equation for the rate of change of  $X$  in which the parameters, such as production and removal rates, vary slowly and depend on age  $\tau$ . The model also includes stochastic noise. Thus,

$$\frac{dX}{dt} = \text{production} - \text{removal} + \text{noise}$$

The model that best describes the data is biologically plausible. The production rate of X rises linearly with age, as  $\eta\tau$ . This aligns with the biological expectation, discussed in the previous lecture, that senescent cells arise from mutant stem cells S' that produce damaged differentiated cells D' that become senescent cells. The number of mutant stem cells rises linearly with age, because stem cell divisions occur at a nearly constant rate across adulthood, and thus the production rate of senescent cells should also be linear with age:

$$\text{production} = \eta\tau$$

The removal of X is carried out by special repair processes, namely immune cells such as NK cells that kill senescent cells. The NK cells discover senescent cells by means of special marker proteins that senescent cells display on their surface. The NK cells then attach to the senescent cell, and inject toxic proteins to kill it. Mice without functioning NK cells show accelerated aging and large amounts of senescent cells. Other immune cells, including macrophages, also play a role by swallowing up the remains. Possibly other types of immune cells help to remove senescent cells.

If this removal process worked at a constant rate  $\beta$  per senescent cell, the probability unit time to remove each senescent cell would be constant with age. The removal term would thus be  $-\beta X$ . However, such a constant  $\beta$  does not match the data. It would result in a linear rise of X with age, as opposed to the nearly exponential rise observed. To see this linear rise of X with age, the equation is  $\frac{dX}{dt} = \eta\tau - \beta X$ , whose steady-state solution is  $X_{st} = \eta\tau/\beta$ .

Thus, it makes sense from the nearly exponential rise of X that *the removal rate per senescent cell should slow down with age*. Karin tested many mathematical ways for this reduction to occur. The simplest way to model this, which accounts for the four features mentioned above, is to assume that **the removal rate drops with the amount of senescent cells**. In other words, senescent cells inhibit their own removal. Such a drop could be due to several processes: immune cells that remove senescent cells could be down-regulated if they kill too often, or they can become inhibited by factors that the senescent cells secrete. The drop in removal rate can also be simply due to a saturation effect, in which the removing cells become increasingly outnumbered by senescent cells as senescent cell numbers rise. Indeed, NK cell numbers are about constant with age in humans. To model such saturation, we use a Michaelis-Menten form (which is good both for inhibition due to secreted factors and for saturation by large numbers, see solved exercise 10.3)

$$\text{removal} = \frac{\beta X}{k + X}$$

Where  $\beta$  is the maximal senescent cells removal capacity (units of senescent cells/time), and  $k$  is the concentration of  $X$  at which they inhibit half of their own removal rate. The removal rate *per senescent cell* thus drops with senescent cells amounts,  $\frac{\beta}{k+X}$  (Fig 10.7)

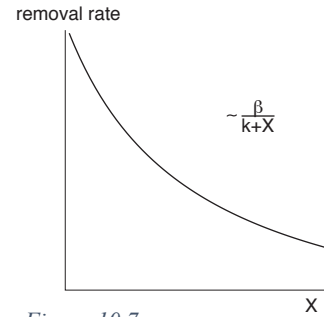


Figure 10.7

Combining production and removal, we obtain a model for the rate of change of  $X$ :

$$\frac{dX}{dt} = \eta\tau - \frac{\beta X}{X + \kappa} \quad [1]$$

Where we use  $\tau$  for age and  $t$  for time to make sure that we understand that there are two timescales: a fast scale (days-weeks) in which damage reaches steady-state, and a slow timescale (years) over which production rate  $\eta\tau$  changes. Note that this model assumes that maximal removal capacity  $\beta$  does not decline with age. Adding such a decline, namely  $\beta(\tau)$ , generally leaves the conclusions the same. For simplicity we ignore this possibility.

Let's compute the steady-state  $X$ . On the fast timescale of weeks, the production rate  $\eta\tau$  can be considered as constant. Setting  $dX/dt = 0$  in Eq. 1 we find that the (quasi-) steady-state  $X$  of is

$$X_{st} \approx \frac{\kappa\eta\tau}{\beta - \eta\tau} [2]$$

Thus,  $X_{st}$  rises linearly with age at first. Then, the term on the bottom becomes closer and closer to zero, which is an explosion point. The rise in  $X$  thus accelerates and diverges at a critical age  $\tau_c = \beta/\eta$  (Fig 10.8). In fact, this rise is almost indistinguishable from an exponential rise over the 5-fold range of the available experimental data (Fig 10.3, Fig 10.8, dashed line). When  $X$  levels rise high enough, they reach levels not compatible with life. Thus, the critical age  $\tau_c = \beta/\eta$  is a rough approximation for the mean lifespan. The lifespan is longer the bigger the repair capacity  $\beta$ , and longer the smaller the rate at which senescent cell production increases with age,  $\eta$ .

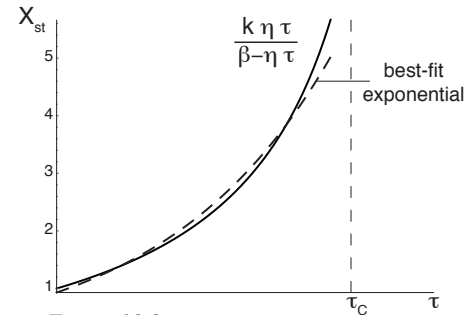


Figure 10.8

To get a graphic sense of why  $X$  accelerates with age, we can use a rate plot. We plot the production and removal terms in Eq 1.

Removal is  $\beta\frac{X}{k+X}$  which is a saturating curve (Fig 10.9). Note that removal rate *per cell* goes down with  $X$  as  $\frac{\beta}{k+X}$ , and the plot

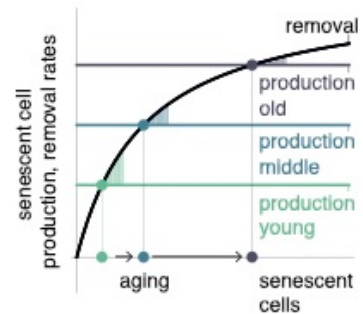


Figure 10.9

shows total removal rate, which is the removal rate per cell times  $X$ , and is therefore a rising and saturating curve.

Production rate, represented by the colored horizontal lines, is low in young organisms and rises with age. The points to watch are where production equals removal. These are the steady-state points at each age. With age, the steady-state  $X$  accelerates to higher and higher levels (Fig 10.9) because of the saturating shape of the removal curve. When the production rises above the removal curve, which occurs when age goes beyond the critical age, the steady state points shifts to infinity, and  $X$  grows indefinitely.

### **Damage production rises with age, and saturates the repair capacity**

Another way to understand this model is the parable of the garbage trucks. A young organism is like a small village that produces a small amount of garbage (senescent cells). The village has 100 garbage trucks, more than enough to clear the garbage. With age, the village becomes a big city producing a lot of garbage. Since we are not designed to be old, there are still 100 trucks. The trucks are overloaded, and garbage piles up in the streets. If there is a perturbation (infection, injury) and extra garbage is added, it stays for a long time. Once garbage is produced at a rate larger than the maximal capacity of the trucks, garbage piles up higher and higher.

Similarly, the body's immune cells that remove senescent cells can get saturated or downregulated, and senescent cells pile up. They cause inflammation, reduce stem cell renewal. The saturation of the immune cells also reduces their ability to do their other tasks: fight infection and cancer. Thus risks of illness and organ dysfunction rises with age.

### **Adding noise to the model explains the variation between individuals in senescent cell levels**

So far, the model does not describe the fluctuations of  $X$  over time for each individual, nor the widening differences between individuals. To understand these stochastic features of the dynamics, we need to add **noise** to the model.

The simplest way to add noise is to add a white-noise term  $\xi$  with mean zero and a variance described by the parameter  $2\epsilon$  (the factor 2 is for convenience in the equations below). This noise describes fluctuations in production and removal due to internal or external reasons such as injury, infection and stress (cortisol). In fact, we don't know what the noise exactly describes. White noise is a convenient way to wrap up our ignorance in a mathematical object that we can work with.

We thus arrive at the main model of this lecture, called the **saturated removal (SR) model**:

$$\frac{dX}{dt} = \eta\tau - \frac{\beta X}{X + \kappa} + \sqrt{2\epsilon}\xi \quad [3]$$

We will use this model to understand the dynamics of senescent cells, and then to understand the origin of the Gompertz law. Let's begin with understanding the variation in  $X$  between individuals at a given age. To do so, we need to compute the distribution of  $X$ ,  $P(X)$ .

---

**Solved example 1: compute the distribution of  $X$  at a given age**

The distribution of  $X$ , denoted  $P(X)$ , is the probability of having  $X$  senescent cells. To derive it, we use an approach analogous to Boltzmann free energy in statistical mechanics or in chemical kinetics. The temperature  $k_b T$  will be the analog of the noise amplitude  $\epsilon$  in the SR model.

To calculate the distribution  $P(X)$ , we use a general method that applies to any stochastic differential equation of the form:  $\frac{dX}{dt} = v(X) + \sqrt{2\epsilon}\xi$ . In the SR model, the 'velocity'  $v(x)$  equals production minus removal, namely  $v(X) = \eta\tau - \beta X/(k + X)$ . The idea is to rewrite the equation using a **potential**  $U(X)$ , defined so that its slope is equal to minus the velocity:  $\frac{dU}{dX} = -v(X)$ .

The potential function can be imagined as a bowl of shape  $U(X)$  (Fig 10.10). The variable  $X$  is like a ball rolling in the bowl (Fig 10.10). The ball rolls down the slope, with velocity  $-v(x)$  that is equal to the slope of the bowl  $dU/dX$ . The bowl is coated with a thick goo (Strogatz, n.d.) and so the ball settles down at the minimum of the bowl without oscillating. At the minimum point slope is zero,  $dU/dX = 0$ , and that is where  $X=X_{st}$ . The steeper the sides of bowl, the

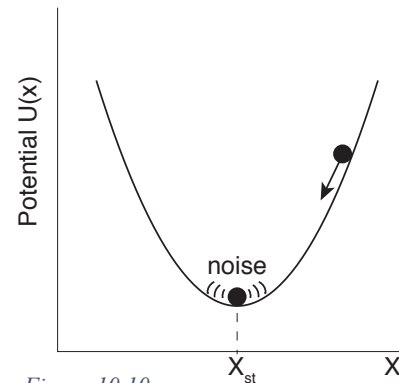


Figure 10.10

faster the ball returns to  $X_{st}$  if it is perturbed. Let's now add noise. Noise jiggles  $X$  near  $X_{st}$ . These jiggles cause a distribution of  $X$  values,  $P(X)$ . Again, the steeper the bowl, the less noise can move  $X$  away from  $X_{st}$ , and the narrower the distribution  $P(X)$ .

The nice thing about the potential-function way of writing the equation is that we can easily compute the steady-state distribution. This distribution  $P(X)$  is given by the Boltzmann distribution, with  $\epsilon$  playing the role of temperature:

$$P(X) \propto e^{-\frac{U(X)}{\epsilon}} \quad [5]$$

An intuitive explanation is provided in solved exercise 10.1. The shallower the bowl, or the larger the 'temperature'  $\epsilon$ , the wider the distribution  $P(X)$ .

For the SR model, the potential  $U(X)$  is

$$U(X) = (\beta - \eta\tau)X - \beta\kappa \log(\kappa + X) \quad [6]$$

Which can be checked by taking  $-dU/dX$  and verifying that it gives

$$\eta\tau - \beta \frac{X}{X+\kappa}.$$

We can safely assume that age  $\tau$  is constant over the fast timescale needed to reach the steady-state distribution  $P(X)$ .

Plotting  $U(X)$  at young and old ages shows that at young ages the bowl is steep, and therefore the distribution is localized around the mean (Fig 10.11). With age, the bowl becomes less and less steep, because its right-hand slope drops as  $-\eta\tau$ . At the critical age, when  $\eta\tau = \beta$ , the bowl opens up and the steady-state goes to infinity.

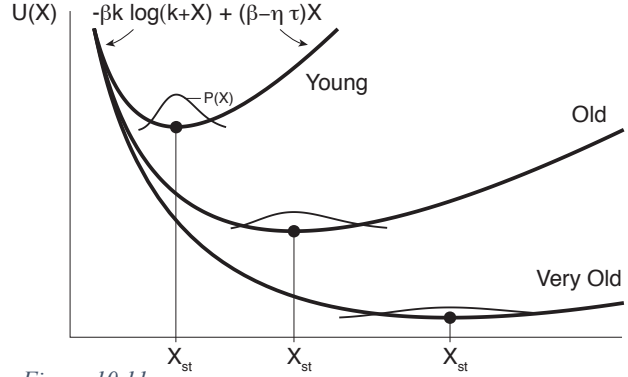


Figure 10.11

Plugging Eq. 6 for  $U(X)$  into the Boltzmann-like law of Eq 5 we obtain the distribution

$$P(X) \propto e^{-\frac{(\beta-\eta\tau)X}{\epsilon}} (\kappa + X)^{\frac{\beta\kappa}{\epsilon}} \quad [6]$$

Which reaches a peak and then falls exponentially with  $X$ . This distribution of senescent cells in the SR model is skewed to the right, and quantitatively matches the skewed distributions observed in the mouse data (Fig 10.5, red lines).

This distribution, by the way, provides a slightly more accurate estimate for the average  $X$ ,

$$\langle X \rangle \approx \frac{\kappa\eta\tau + \epsilon}{\beta - \eta\tau} \quad [7]$$

Which rises with age (Fig 10.8, red line). The standard deviation of  $X$  also rises with age and diverges at  $\tau_c$ , as shown by calculating the std of  $P(X)$ :

$$\sigma \approx \frac{\sqrt{\kappa\beta + \epsilon^2}}{\eta\tau - \beta} \quad [8]$$

This rise in std matches the observed rise with age of the standard-deviation of the light emitted from the mice of Burd et al (Fig 10.1). The SR model even captures the fact that variation rises more slowly than the mean, such that the ratio between average and std rises linearly with age observed as in the mouse senescent-cell data

$$\frac{\langle X \rangle}{\sigma} \approx \frac{\kappa\eta\tau + \epsilon}{\sqrt{\kappa\beta + \epsilon^2}} \sim \tau.$$



The SR model also explains the increasing correlation times with age. At young ages, the bowl is steep. Thus, if  $X$  is away from  $X_{st}$ , it returns to  $X_{st}$  quickly (Fig 10.12). At old ages, in contrast, the bowl is almost completely flat. The trajectory of the ‘ball’ is dominated by noise, with very little restoring force coming from the steepness of the bowl

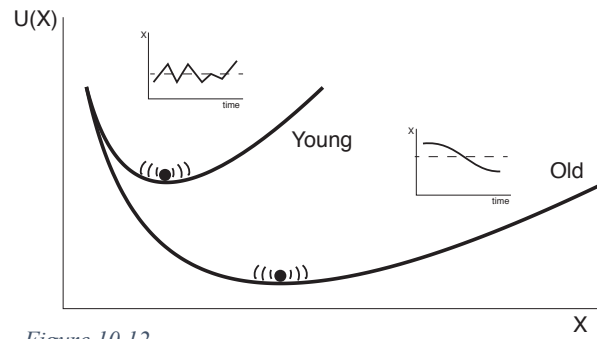


Figure 10.12

(Fig 10.12). Hence individuals that stray away from  $X_{st}$  have a slower restoring force back to the mean, and stay away for longer times.

Such increasing correlation times have a general name in physics, “**critical slowing down**”. They are a mark of an approaching phase transition. In our case, the phase transition is to infinite  $X$ , which is death. In the classical example of a phase transition, the boiling of water, large and slow fluctuations in density can be seen near the boiling point. In other areas of science, slowing down of fluctuations can be a warning sign of a big transition. Examples include climate fluctuations before an ice age, or ecological fluctuations before a species extinction [Schaffer 2009].

The mouse data allows estimating all four model parameters,  $\eta$ ,  $\beta$ ,  $k$  and  $\epsilon$ . The best fit parameters are approximately  $\eta = 4 \cdot 10^{-4} \text{ days}^2 \sim 0.15/\text{year}/\text{day}$ ,  $\beta = 0.3/\text{day}$ ,  $k = 1$ ,  $\epsilon = 0.1$ , in units where the average senescent cells in young mice is 1. The rough estimate of lifespan  $\tau_c = \frac{\beta}{\eta} \sim 2 \text{ years}$  is about right for mice. These parameters give a concrete prediction for the half-life of a senescent cell. The half-life is about 5 days in young mice, and rises to about a month in old mice (25 days in 22 month old mice).

**An experimental test shows that senescent cells are removed in days from young mice but in weeks from old mice**

This prediction was interesting enough to test experimentally. We teamed up with Valery Krizhanovsky, a senescent cell researcher from our department, and his PhD student Amit Agrawal. The idea was to induce extra senescent cells in mice, and then to measure how quickly the senescent cell levels go back to steady state (Fig 10.13).

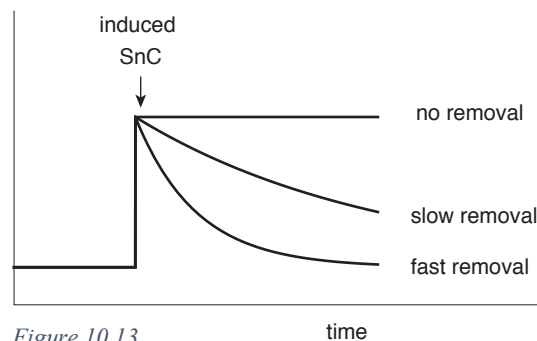


Figure 10.13

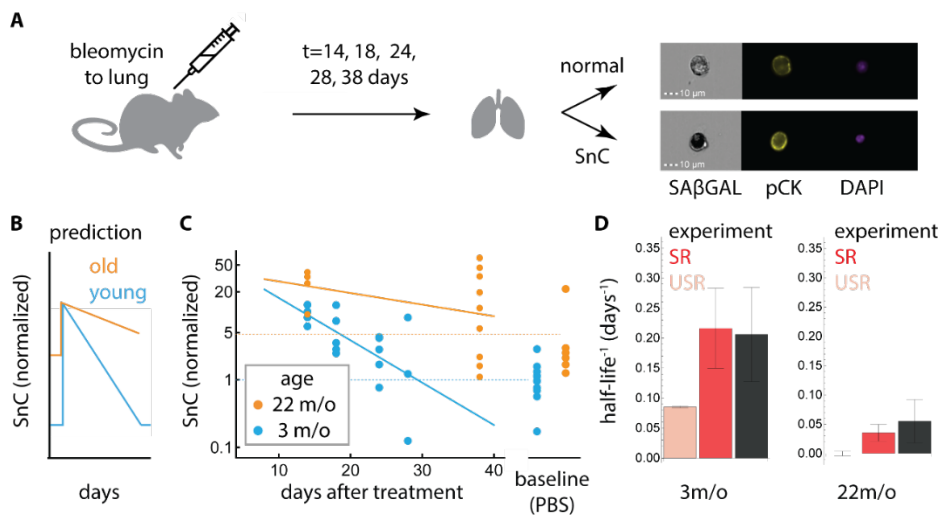


Figure 10.14

Krizhanovsky used a drug, called Bleomycin, which induces DNA damage which makes cells become senescent cells. The drug was introduced into the lungs of mice. The drug is cleared away within a day. Due to the DNA damage, after 5 days, the lungs are full of senescent cells. Then, mice were killed at various timepoints, and the amount of senescent cells in their lungs was measured; the lung was dissolved into single cells, which were stained with a dye that labels senescent cells (called SA-beta-gal). The individual cells were photographed in a machine called an imaging flow-cytometer (Fig 10.14A), and the number of senescent epithelial lung cell were counted.

In young mice, the senescent cells half-life was  $5 \pm 1$  days (Fig 10.14C). In old mice (22-month-old), removal was much slower, with an estimated half-life of about a month. Note the variation in senescent cells between the old mice. These measurements agree well with the predictions of the SR model (Fig 10.14D). The agreement is striking because the SR model was calibrated on the luciferase-mice, with a different marker for senescent cells (p16 versus SA-beta gal), and a different system (whole body versus lung). This agreement adds confidence in the prediction of the SR model that removal of senescent cells slows with age.

### Gompertz mortality is found naturally in the SR model

In the remainder of the lecture, we explore the implications of rapid senescent cells turnover and slowdown of removal for the question of variability in mortality. As we saw in the previous lecture, lifespan varies even in inbred organisms raised in the same conditions, demonstrating a non-genetic component to mortality. In many species, including mice and humans,

risk of death rises exponentially with age, the Gompertz law, and decelerates at very old ages (Fig 10.15).

To connect senescent cells dynamics to mortality, we need to know the relationship between senescent cell abundance and the risk of death. The precise relationship is currently unknown. Clearly, senescent cells abundance is not the only cause for morbidity and mortality. It does, however, seem to be an important causal factor because removing senescent cells from mice increases mean lifespan, and adding senescent cells to mice increases risk of death and causes age-related decline.

Let's therefore explore the simple possibility that death can be modeled to occur when senescent cell abundance exceeds a threshold level  $X_c$ . The threshold represents a collapse of an organ system or a tipping point such as sepsis (Figure 10.16). Thus, death is modelled as a **first-passage time process**, when senescent cells cross  $X_c$ . We use this threshold-crossing assumption to illustrate a way of thinking, because it provides analytically solvable results. Other dependencies between risk of death and senescent cells abundance, such as Hill-functions with various degrees of steepness, provide similar conclusions.

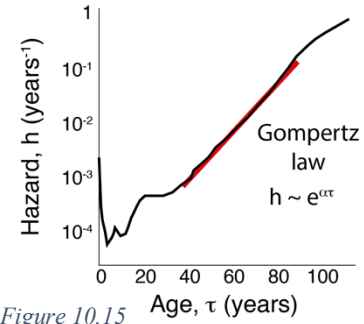


Figure 10.15

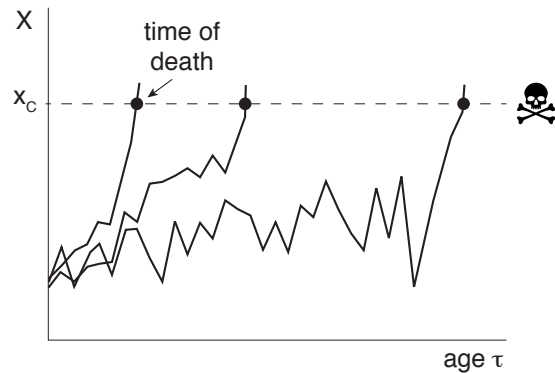


Figure 10.16

**Solved exercise 2: Show that the SR model gives the Gompertz law of mortality.**

To estimate the probability that  $X$  crosses the death-threshold  $X_c$ , we apply an approach which is analogous to the rate of a chemical reaction crossing an energy barrier  $\Delta G$ . This rate is the Boltzmann factor  $\exp(-\frac{\Delta G}{k_B T})$ . As always, in our case the noise amplitude  $\epsilon$  plays the role of temperature  $k_b T$ , and the energy barrier is the difference between the potential  $U$  at  $X_c$  and at the steady-state value  $X_{st}$ ,  $\Delta G = U(X_c) - U(X_{st})$ . Thus, the probability for  $X$  crossing  $X_c$ , namely the risk of death that we call the hazard, is

$$h \approx e^{-\frac{U(X_c) - U(X_{st})}{\epsilon}}$$

This equation is called Kramers equation in the field of stochastic processes. An intuitive explanation is that the ball in the well needs to climb a potential difference of  $\Delta U = U(X_C) - U(X_{st})$  in

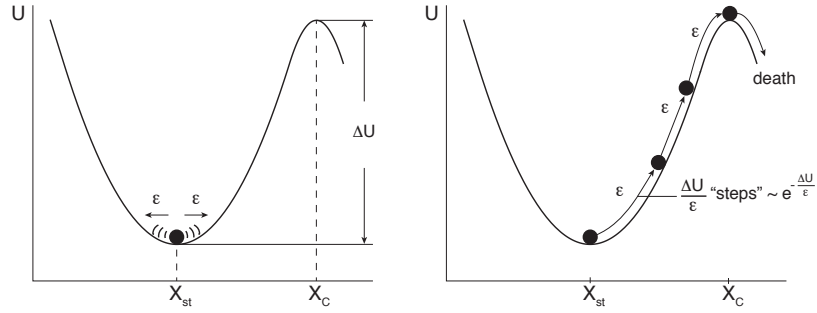


Figure 10.17

order to fall off into the death region (Fig 10.17). It needs to climb using ‘kicks’ provided by the noise, each of size epsilon. Each noise kick can be either to the right or left. Since you need  $\frac{\Delta U}{\epsilon}$  kicks, all in the right direction, the chance is exponentially small and goes as  $e^{-\frac{\Delta U}{\epsilon}}$ .

The potential  $U$  in our model is given by Eq.3. For the Gompertz law to hold, one needs the term  $\frac{U(X_C) - U(X_{ST})}{\epsilon}$  to decrease linearly with age  $\tau$ , so that  $h \approx e^{\alpha\tau}$ .

The exponent of the hazard rate in the SR model indeed shows the required linearity in time, in bold in the equation:

$$-\frac{U(X_C) - U(X_{ST})}{\epsilon} = \frac{(\kappa + X_C)\eta\tau - X_C\beta + \kappa\beta \cdot \text{Log} \left[ \frac{(\kappa + X_C)(\beta - \eta\tau)}{\kappa\beta} \right]}{\epsilon} \quad [8]$$

We thus find that, up to a prefactor that does not depend on age:

$$h(\tau) \approx (\beta - \eta\tau)^{\frac{\kappa\beta}{\epsilon} + 1} e^{\frac{(\kappa + X_C)\eta\tau}{\epsilon}} \quad [9]$$

This is a big moment. The hazard rises exponentially with time as  $e^{\alpha\tau}$  with an exponent  $\alpha$ , called the Gompertz ageing rate, given by

$$\alpha = \frac{(\kappa + X_C)\eta}{\epsilon}$$

The Gompertz ageing rate parameter (such as the 8-year doubling time in humans) can thus be written in terms of molecular parameters.

This solution also shows a deceleration in the rise of the hazard rate at very old ages (when  $\eta\tau \approx \beta$ ), due to the prefactor  $(\beta - \eta\tau)^{\frac{\kappa\beta}{\epsilon} + 1}$ . This slowdown in hazard is observed in the empirical hazard curves. Note that this approximation begins to be inaccurate when  $\eta\tau > \beta$ , and simulations of the full SR model are needed to compute the hazard curve at old ages. Simulations show that rise of

the hazard continues to slow with age. Other models usually do not show the Gompertz-law in their first passage time solution (Exercises).

The SR model analytically reproduces the Gompertz law, including the observed deceleration of mortality rates at old ages (Fig 10.18). The SR model gives a good fit to the observed mouse mortality curve using parameters that agree with the experimental half-life measurements and longitudinal senescent cells data. The threshold for death is  $X_C = 17 \pm 2$ , meaning that the threshold  $X_C$  is about 17 times larger than the mean senescent cell level in young individuals. Thus, turnover

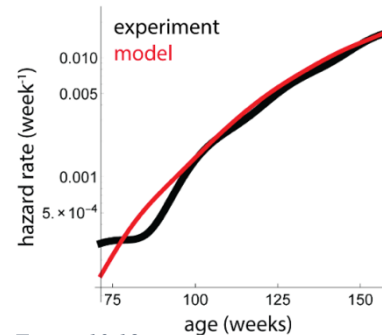


Figure 10.18

of days in the young and weeks in the old provides senescent cells variation such that individuals cross the death threshold at different times, providing the observed mortality curves.

The SR model can address the use of drugs that eliminate senescent cells, known as senolytic drugs. To reduce toxicity concerns, it is important to establish regimes of low dose and large inter-dose spacing. The model provides a rational basis for scheduling senolytic drug administrations. Specifically, treatment should start at old age, and can be as infrequent as the Senescent cells turnover time (~month in old mice) and still be effective.

### Turnover of days in young and weeks in old can explain human Gompertz law

Let's use the results from the mouse data to study human mortality curves. In humans, mortality has a large non-heritable component (estimated at 80%) and hence we can assume that the parameters eta, beta k and epsilon are similar between people and that much of the variation is due to stochastic effects. A good description of human mortality data, corrected for extrinsic mortality, is provided by the same parameters as in mice, except for a 60-fold slower increase in senescent-cell production parameter  $\eta$  with age in the human parameter set (Figure 10.19).

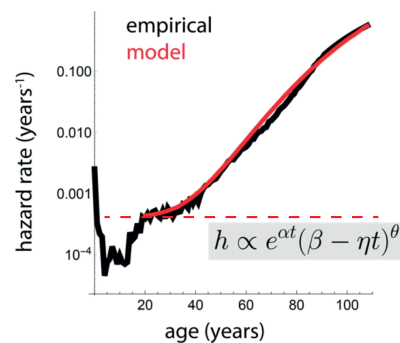


Figure 10.19

This slower increase in senescent cell production rate can be due to improved DNA maintenance in humans compared to mice. Perhaps this parameter  $\eta$  is the main way that evolution tunes lifespan of different mammals, as in the mass-longevity triangle of the previous lecture. Indeed, long-lived animals such as elephants and naked mole rats have enhanced repair processes for DNA damage compared to mice. We conclude that the critical slowing-down described by the

SR model provides a possible cellular mechanism for the variation in mortality between individuals.

### **Similar considerations can explain aging statistics in model organisms**

The SR model can be generalized beyond senescent cells. It should apply to any form of damage that whose production rises with age and whose removal becomes saturated. We therefore explore the SR model to understand key experiments in model organisms without senescent cells such as the fruit fly *Drosophila melanogaster* and the worm (or more correctly the nematode) *C. elegans*. The advantage of these model organisms is that interventions that affect lifespan can be studied with excellent statistics in lab conditions. Thus, let's consider  $X$  as a damage that is causal for aging, that accumulates with age and has SR-type dynamics, namely turnover that is much more rapid than the lifetime, rising production rate and self-slowing removal. Clues for the identity of such factors may be gene-expression variations in young organisms that correlate with individual lifespan, and the actions of genes that modulate lifespan.

### **Rapid shifts between hazard curves in Fruit flies**

Work in *C. elegans* and *Drosophila* provides constraints to test the SR model. For example, in a classic paper, (Mair, Goymer, Pletcher, & Partridge, 2003). measured the effect of two lifespan-extending interventions in *Drosophila*, lifespan-extending diets (LE) and temperature change, when applied at mid-adulthood. They found that the interventions had different effects on lifespan: (i) LE led to rapid switches in mortality rate, and (ii) changing temperature affected the slope of the mortality rate.

These results can be explained by the SR model with rapid turnover. A relatively rapid turnover for *Drosophila* means turnover on the order of minutes to hours. We therefore set  $\beta = 1 \text{ hr}^{-1}$ ,  $\kappa = 1$ , and  $\epsilon = 1 \text{ hr}^{-1}$ . To fit the survival curve for fully fed flies obtained by (Mair et al., 2003) we set  $\eta = 0.03 \text{ hr}^{-1} \text{ day}^{-1}$ , and death when  $X > X_C$  with  $X_C = 15$ . Flies on life extending diet (LE) are fit by a lower value,  $\eta = 0.02 \text{ hr}^{-1} \text{ day}^{-1}$ . Note that the purpose here is to demonstrate that the SR model can capture the behavior of the data, and not to provide accurate estimates for the parameters (the data is insufficient to pin down the parameters).

The hazard curve for the life-extending (LE) diet can be explained by assuming that it changes any of the model parameters. For example, LE can change  $\eta$  in a reversible manner (Figure 10.20 A), and hence affect the rate of damage production  $p$ . In this case, changing diet leads to damage production  $p(t) = \eta_1 \tau$ , where  $\eta_1$  is the rate of increase in damage production of the current diet. The rapid turnover of damage rapidly reverts the mortality rates when diet changes (Figure 10.20 A). More generally, LE may change any parameter of the SR model, including removal rate  $\beta$ , as long as the effect on the parameter is reversible.

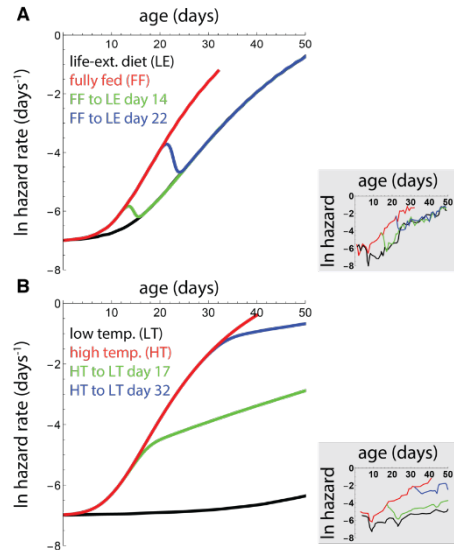


Figure 10.20

On the other hand, the temperature intervention can be explained by assuming that it affects an underlying damage accumulation rate that sets  $\eta$  (10.20 B), that is, temperature multiplies  $\frac{dp}{d\tau}$ . Changing temperature at age  $\tau'$  therefore leads to damage production  $p(\tau) = \eta_0 \tau' + \eta_1(\tau - \tau')$ , where  $\eta_0$  was the previous rate of increase in damage production and  $\eta_1$  the rate after temperature change. This intervention affects the slope of increase in mortality rate with age, but does not revert the mortality rates (Fig 10.20 B).

### C elegance scaling data

A further test is whether the SR model can explain the scaling of survival curves for *C. elegans* under different life-extending or life shortening genetic, environmental and diet perturbations. These perturbations change lifespan by an order of magnitude, but the survival curves collapse on the same curve when age is scaled by mean lifespan (Figure 10.21 insets), as discovered in an elegant experiment by (Stroustrup et al., 2016). The SR model provides this **scaling**, to a very good approximation, for perturbations that affect the accumulation rate  $\eta$  (Figure 10.21 A). Interestingly, there is no scaling when a perturbation affects other parameters such as removal rate  $\beta$  or noise  $\epsilon$  (Fig 10.21 B, D), a prediction that may apply to exceptional perturbations in which scaling is not found such as the *eat-2* and *nuo-6* mutations. In all cases, scaling cannot be found in models without rapid turnover. We conclude that the SR model of rapid turnover with critical-slowness is a candidate explanation for scaling of survival curves in *C. elegans*.

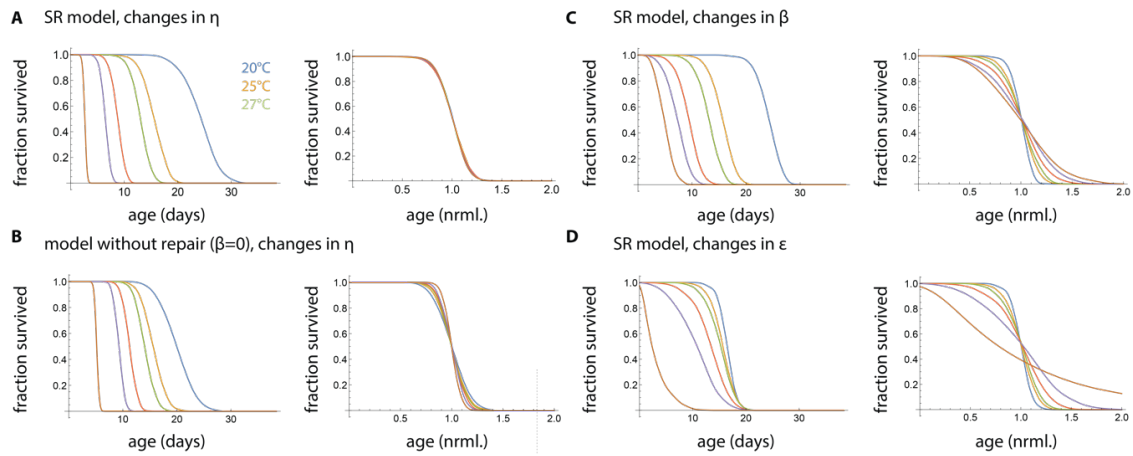


Figure 10.21

### Approaches to slow down aging and aging-related diseases:

Current medicine focuses on treating each age-related disease - diabetes, cancer, heart disease and so on. A different approach would be to deal with their shared risk factor - to slow the aging process, or more precisely to slow the rise of senescent cells (and other aging-related damage). This is the **Geroscience hypothesis**: slowing the core process of ageing will prevent and improve many age related diseases.

The conceptual framework we discussed points to two general strategies: reduce production rate  $\eta$  or increase removal capacity  $\beta$ .

Reducing production can be achieved by boosting cellular damage-repair systems. One way to achieve this is calorie restriction and other types of restricted feeding. Starvation seems to shift the balance from growth towards maintenance, and upregulate damage repair mechanisms in cells. A large effort is devoted to develop drugs that mimic calorie restriction by, for example, perturbing the IGF1 pathway. One promising drug is metformin, used for treating diabetes since the 1920s. Metformin inhibits the IGF1 pathway, and seems to tip the balance between growth and repair towards more repair. An encouraging sign is that people taking metformin have lower risks of cancer. A current effort is to convince the federal food and drug administration (FDA) to allow clinical trials for aging (currently only trials for a specific disease are allowed). Metformin is one suggested drug for such a trial, along with other inhibitors such as rapamycin.

Increasing the removal of senescent cells is also an attractive possibility. That is what **senolytic drugs** do. Senolytics remove senescent cells by exploiting the Achilles heels of senescent cells that are not found in most other cells. There are several families of senolytics, and some have entered clinical trials in humans in 2019 for diseases such as idiopathic pulmonary fibrosis and osteoarthritis.

Another approach is target the factors that senescent cells secrete, such as pro inflammatory factors.



Finally, immune-based strategies can potentially increase removal capacity beta. This year (2020), an immune approach developed to fight cancer cells was repurposed to remove senescent cells in mice. In this approach, called CAR-T, killer T-cells are taken from the mouse and genetically engineered to express a T-cell receptor that recognizes a protein found only on the surface of senescent cells. These T-cells are re-introduced into the mice and kill senescent cells.

A sobering note for fantasies about immortality. Even if one removes senescent cells, the organism will still get sick and die eventually. For example, mutant stem cells produce damaged cells in all tissues, D'. Many of these damaged cells do not become senescent, but do have reduced function. As the fraction of damaged cells increases, the reduced function will eventually cause an organ system to fail. Studies show that aged individuals have on the order of 1000 mutations in each of their cells. Their organs like the skin, gut and lung are made of little local 'kingdoms' of cells, each from a different clone of stem cells, each kingdom with its individual random mutations. In about 10% of aged people, for example, all blood cells are made from one or a few stem cell clones in the bone marrow. Blood health depends on the luck of which mutations these stem cells have. Thus, although senescent cells are a major component, other damaged cells are likely to be important for aging.

The research into removing senescent cells has been accelerating in the past 4 years. As we have learned from past breakthroughs in biology, reality holds unexpected challenges, and initial promise usually doesn't fully materialize. We don't know if there will be a pill you can take in middle age that will make you younger. But there are so many avenues to try that it's likely that such a pill will help at least some people with some illnesses. These are exciting times.

### Exercises:

#### Solved exercise 10.1: Intuitive derivation of 'Boltzmann-like' form of the steady-state distribution:

Consider a stochastic process of the form  $\frac{dx}{dt} = v(x) + \sqrt{2\epsilon}\xi$ . The function  $v(x)$  is called the velocity of  $x$ . In the SR model, we have a velocity equal to production minus removal:  $v(x) = \eta t - \frac{\beta x}{k+x}$ . Define the potential  $U(x)$  by  $\frac{dU}{dx} = -v(x)$ . Explain intuitively why, at steady-state, the probability distribution is  $P(x) = P_0 \exp\left(-\frac{U(x)}{\epsilon}\right)$ .

**Solution:** Consider a large number of particles moving along a one-dimensional pipe. They diffuse with diffusion coefficient  $\epsilon$  and are also swept along the pipe by a velocity field  $v(x)$ . The particle density at steady-state is  $P(x)$ . The flux at point  $x$  due to the velocity field is the velocity times the density:  $v(x)P(x)$ . The flux due to diffusion can be found by Fick's law of diffusion, which shows

a diffusive flux from high to low densities proportional to the gradient:  $-\epsilon dP/dx$ . At steady-state total flux is zero, so that the two fluxes must sum to zero:  $v(x)P - \epsilon dP/dx = 0$ . Thus,  $\frac{dP}{dx} = \frac{v(x)P(x)}{\epsilon}$ . The solution is  $P(x) = P_0 \exp\left(-\frac{U(x)}{\epsilon}\right)$ . Thus, at steady-state, in regions where velocity is large the density  $P(x)$  shows a steep opposing slope so that diffusion flux can balance velocity flux.

### 10.2. Survival and hazard functions:

(a) Show that hazard,  $h(\tau)$ , defined as the probability of death per unit time, is related to survival  $S(\tau)$  as follows

$$h(\tau) = -\frac{1}{S} \frac{dS(\tau)}{d\tau} = -\frac{d \log S(\tau)}{d\tau}$$

(b) Show that  $S(\tau) = e^{-\int h(\tau) d\tau}$

(c) What is the survival function  $S$  when the hazard follows the Gompertz-law? Plot this survival function.

(d) What is the survival function if hazard is constant  $h(\tau) = h_0$ ?

(e) A tree has a hazard function that drops with age,  $h(\tau) = \frac{a}{1+b\tau}$ . What is the survival function? Plot and compare to d and c. What might be a biological cause of such a decreasing hazard function?

**10.3 Removal of Senescent cells based on saturating their own removal process:** Senescent cells are removed by immune cells such as NK cells, which we will denote by  $R$ . There are a total of  $R_T$  removing cells in the body, and that this number does not change appreciably with age (as is indeed the case for NK cells in humans). The  $R$  cells meet Senescent cells, denoted  $X$ , at rate  $k_{on}$  to form a complex  $[R X]$  which can either fall apart at rate  $k_{off}$ , or end up killing the Senescent cells at rate  $v$ . Thus,  $R+X \leftrightarrow [RX] \rightarrow R$ .

(a) Explain the following dynamic equation for the complex:

$$\frac{d[RX]}{dt} = k_{on} R X - (v + k_{off})[RX]$$

(b) Use the fact that  $R$  cells can be either free or in a complex, so that  $R + [RX] = R_T$ , to show that the removal rate of Senescent cells is

$$removal = \frac{\beta X}{k + X}$$

(c) What are the values of the maximal removal capacity  $\beta$ , and the half-way saturation point  $k$ ? Explain intuitively.

**10.4 No repair:** Consider an accumulation process of damage with constant production and no removal

$$\frac{dX}{dt} = \eta + \sqrt{2\epsilon}\xi .$$

- What is the mean damage  $X$  as a function of age?
- What is the distribution  $P(X)$ ?
- What is the hazard assuming that death occurs when  $X > X_c$ ? Is there a Gompertz law?

**10.5 Age-dependent reduction in repair capacity:** Consider a process in which damage is produced at a constant rate  $\eta$ , and removal does not saturate. Removal rate per cell drops with age,

$$\frac{dX}{dt} = \eta + (\beta - \beta_1\tau)X + \sqrt{2\epsilon}\xi .$$

- What is the mean damage  $X$ ?
- What is the distribution  $P(X)$  at age  $\tau$ ?
- What is the ratio of mean and standard deviation of  $X$ :  $\langle X \rangle / \sigma$ ?
- What is the hazard, assuming that death occurs when  $X > X_c$ ? Is there a Gompertz law?

**10.6 Deterministic model:** Assume that the Gompertz law arises not from stochastic effects, but instead from individual differences, set a birth, in  $X$  production and removal parameters, in which each individual  $i$  has its own noise-free equation  $\frac{dX}{dt} = \eta_i - \beta_i X$ . Death is modelled when  $X$  crosses threshold  $X_c$ . What distribution of production and removal parameters  $\eta_i, \beta_i$  can provide the Gompertz law? What features does this model not explain?

**10.7** What is the effect on the hazard curve of the SR model of a change in each of the parameters  $\beta, \eta, \epsilon, k$ ? Plot examples of hazard curves to demonstrate your answer.

**10.8 Senescent cell half-life:** show that in the SR model, the half-life of a senescent cell is

$$t_{1/2} = \log(2)(k\beta + \epsilon) / \beta(\beta - \epsilon\tau)$$

**10.9 Critical slowing down:** Read (Scheffer et al., 2009).

- How does critical slowing down relate to the SR model?
- Suggest a phenomenon beyond those discussed in Scheffer which might show critical slowing down, and suggest an experiment or measurement to test this.

**10.10 (Challenging question) General model:** Damage is produced at rate  $\eta(X, \tau)$  and removed at rate  $\beta(X, \tau)$ . The equation is  $\frac{dX}{dt} = \eta(X, \tau) - \beta(X, \tau) + \sqrt{2\epsilon}\xi$

- (a) What is the steady-state distribution at age tau?
- (b) What is the risk of death as a function of age, modelled by first passage time of a threshold  $X_c$ ?
- (c) Under which conditions does risk of death go as the Gompertz law?

**10.11 Strehler and Mildvan (1960) model for the Gompertz law.** Strehler and Mildvan (STREHLER & MILDVAN, 1960) (SM) proposed a phenomenological process for the Gompertz law. Organisms are assumed to start with an initial survival capacity, termed  $V$ , declining linearly with age  $x$  as  $V(x) = V_0(1 - Bx)$ , where  $B$  indicates the fraction of vitality loss per unit time. Over life, animals experience random external challenges or insults with a mean frequency  $K$ . Challenges have random magnitudes, exponentially distributed with an average magnitude  $D$  that expresses the average deleteriousness of the environment. Death occurs when the magnitude of a challenge exceeds the remaining vitality. A detailed review of the SM theory can be found in Finkelstein (2012). (Finkelstein, 2012).

- (a) Show that these assumptions produce the Gompertz law  $h(\tau) = ae^{b\tau}$ . Calculate  $a$  and  $b$ .
- (b) What similarities and differences does this theory have with the SR model?

**10.12 Stem cell therapy:** Would adding young stem cells to an aged organism help to address aging, according to the conceptual picture in this lecture? What are your thoughts (100 words).

### Reference:

- Burd, C. E., Sorrentino, J. A., Clark, K. S., Darr, D. B., Krishnamurthy, J., Deal, A. M., ... Sharpless, N. E. (2013). Monitoring tumorigenesis and senescence in vivo with a p16 INK4a-luciferase model. *Cell*, *152*(1–2), 340–351. <https://doi.org/10.1016/j.cell.2012.12.010>
- Finkelstein, M. (2012). Discussing the strehler-mildvan model of mortality. *Demographic Research*. <https://doi.org/10.4054/DemRes.2012.26.9>
- Mair, W., Goymer, P., Pletcher, S. D., & Partridge, L. (2003). Demography of dietary restriction and death in *Drosophila*. *Science*, *301*(5640), 1731–1733. <https://doi.org/10.1126/science.1086016>
- Scheffer, M., Bascompte, J., Brock, W. A., Brovkin, V., Carpenter, S. R., Dakos, V., ... Sugihara, G. (2009). Early-warning signals for critical transitions. *Nature*. <https://doi.org/10.1038/nature08227>
- STREHLER, B. L., & MILDVAN, A. S. (1960). General theory of mortality and aging. *Science*, *132*(3418), 14–21. <https://doi.org/10.1126/science.132.3418.14>
- Strogatz, S. H. (Steven H. (n.d.). *Nonlinear dynamics and chaos : with applications to physics, biology, chemistry, and engineering*.
- Stroustrup, N., Anthony, W. E., Nash, Z. M., Gowda, V., Gomez, A., López-Moyado, I. F., ... Fontana, W. (2016). The temporal scaling of *Caenorhabditis elegans* ageing. *Nature*. <https://doi.org/10.1038/nature16550>